Published in final edited form as:
Arch Ophthalmol. 2010 February ; 128(2): 212. doi:10.1001/archophthalmol.2009.395.

Development of Choroidal Neovascularization in rats with Advanced Intense Cyclic Light-induced Retinal Degeneration

Daniel M. Albert, MD, MS[1], **Aneesh Neekhra, MD**[1], **Shoujian Wang, MD, PhD**[1], **Soesiawati R. Darjatmoko, BS**[1], **Christine M. Sorenson, PhD**[2], **Richard R. Dubielzig, DVM**[3], and **Nader Sheibani, PhD**[1,4,*]

[1] Department of Ophthalmology & Visual Sciences, University of Wisconsin School of Medicine and Public Health, Madison, WI

[2] Department of Pediatircs, University of Wisconsin School of Medicine and Public Health, Madison, WI

[3] Department of Veterinary Medicine, University of Wisconsin School of Medicine and Public Health, Madison, WI

[4] Department of Pharmacology, University of Wisconsin School of Medicine and Public Health, Madison, WI

Abstract

Objective—To study the progressive changes of intense cyclic light-induced retinal degeneration and determine whether it results in choroidal neovascularization (CNV).

Methods—Albino rats were exposed to 12 h of 3000 lux cyclic light for 1, 3, or 6 months. Prior to euthanization, fundus examination, fundus photographs, fluorescein and indocyanine green angiography, and Optical Coherence Tomography (OCT) evaluations were performed. Light exposed animals were euthanized after 1, 3, or 6 months for histopathological evaluation. Retinas were examined for the presence of 4-hydroxy-2-nonenal (HNE) and nitrotyrosine modified proteins by immunofluorescence staining.

Results—Chronic intense cyclic light exposure resulted in retinal degeneration with loss of the outer segments of photoreceptors and approximately two-thirds of the outer nuclear layer (ONL) and development of sub-retinal pigment epithelium (RPE) neovascularization after 1 month. Almost the entire ONL was absent with the presence of CNV, which penetrated Bruch's membrane and extended into the outer retina after 3 months. Absence of the ONL, multiple foci of CNV, RPE fibrous metaplasia, and connective tissue bands containing blood vessels extending into the retina were observed after 6 months. All intense light exposed animals showed an increased presence of HNE and nitrotyrosine staining. OCT and angiographic studies confirmed retinal thinning and leakiness of the newly fromed blood vessels.

Conclusions—Our results suggest albino rats develop progressive stages of retinal degeneration and CNV after chronic intense cyclic light exposure allowing the detailed study of the pathogenesis and treatment of age-related macular degeneration.

*Corresponding Author: Nader Sheibani, PhD, University of Wisconsin, Department of Ophthalmology and Visual Sciences, 600 Highland Avenue, K6/458 CSC, Madison, WI 53792-4673, nsheibanikar@wisc.edu, Tel 608-263-3345 Fax 608-265-6021.

Introduction

Age-related macular degeneration (AMD) is the leading cause of blindness in humans in developed countries (1–3). AMD is characterized by progressive degeneration of the macula, usually bilateral, leading to a severe decrease in vision and a central scotoma. The decrease in vision results either from retinal degeneration, called geographic atrophy (i.e., dry or nonexudative AMD), or from the secondary effects of choroidal neovascularization (CNV) (i.e., wet or exudative AMD) (4). Although changes in choroidal capillaries are observed in both nonexudative and exudative AMD, the etiology of the two types of AMD may be distinct. The retinal pigment epithelium (RPE) atrophy was recently described to be the initial insult in nonexudative AMD, while changes in choroidal capillaries preceded the RPE atrophy in exudative AMD (5). However, the impact of changes in RPE on retinal and choroidal vasculature requires further elucidation. Animal models of AMD that manifest some of the features of human AMD have become available in the recent years (6). However, most of these models do not represent the full spectrum of the pathologic changes observed in human AMD (7,8). Animal models that mimic the complex and progressive characteristics of AMD are extremely valuable for studying the pathogenesis of AMD and testing different treatment modalities.

The pathogenesis of AMD is not fully understood, but exposure to light is reported in epidemiological studies to be a risk factor for AMD in humans (9). Light energy is essential for visual function, but in excessive amounts produces photochemical damage to retinal neurosensory cells. In 1966, Noell et al. published an early histological study of retinal damage by light in rats. They documented the loss of photoreceptor and outer nuclear layers in albino rats after exposing them to constant light for periods ranging from a few hours to a few days (10). Subsequent light and electron microscopic studies revealed the sequence of histological events leading to the disappearance of photoreceptors and complete RPE- Müller cell adhesion (11,12) and RPE neovascularization by retinal capillaries (13–15).

Kremers et al. in 1988 proposed two classes of photochemical damage of retina, depending on the level of irradiance of exposed white light. In Class 1, with low irradiance, the initial damage is restricted to photoreceptors, while in class 2, with high irradiance, the RPE is the site of first insult (16). The rate and extent of retinal degeneration were increased with an increase in the duration and intensity of light exposure (12,17). The appearance of the albino rat retina remained normal after 1 h of 2,500 lux intensity light exposure, while pyknotic changes in the outer nuclear layer were noted when light exposure increased to 4 h (10). Additionally, O'Steen reported that the susceptibility to light damage in the rat increases markedly at 16–24 weeks compared to 3–4 weeks of age with approximately 95% loss of photoreceptors (18).

The exact molecular events involved in the light induced retinal degeneration have not been fully determined. However, formation of reactive oxygen species (ROS) and consequent oxidative damage to retinal cells is one of the proposed mechanisms (9,10,19–21). It is also suggested that the formation of bleached products of rhodopsin or other visual pigments leads to the formation of phototoxic molecules that mediate retinal cytotoxicity (22,23). Both the caspase-dependent and caspase-independent pathways are involved in light induced apoptosis of photoreceptors (24,25). In recent years, vision scientists have increasingly utilized light induced retinal degeneration in rodents for pathogenetic and therapeutic studies following chronic light exposure for a period of a month or more. However, the advanced stages of intense cyclic light-induced retinal degeneration have not been previously evaluated.

Chronic light-induced ROS can damage Bruch's membrane and may stimulate CNV by fostering a "proangiogenic" environment in the retina (21,26). Numerous studies reported RPE neovascularization in various retinal degeneration models which arises from the inner retinal

capillaries, with minimal contribution from the choroid vasculature, and, may be influenced by the rate at which photoreceptors degenerate (13,14). However, the accumulation of lipofuscin in RPE cells is, at least in part, also related to light exposure (27). Lipofuscin deposition contributes to the formation of large confluent drusen and pigmentary changes in the RPE layer, is also thought to lead to the development of CNV (28). Thus, the relative contributions of the neurosensery retina and RPE degeneration to the development of CNV in the aging eye clearly require further study.

Based on the published work of others and our own previous observations of light induced retinal degeneration in rodents, we hypothesized that rodents with late stage of intense cyclic light induced retinal degeneration develop CNV. To test this hypothesis, we studied the effects of long duration and high intensity cyclic light exposure to the eyes of Wistar and Sprague-Dawley (SD) albino rats. Here we show that exposure to high intensity cyclic light for 1–6 months results in rapid retinal degeneration, which ultimately progresses to CNV, with minimal contribution from retinal capillaries and RPE neovascularization. These changes were associated with increased oxidative stress, as revealed by increased immunostaining for the presence of 4-hydroxy-2-nonenal (HNE), a product of lipid peroxidation (29), and nitrotyrosine modified proteins, a product of peroxynitrate reaction (30). Thus, chronic intense cyclic light exposure of albino animals may provide a suitable model to study the progressive pathogenesis of exudative AMD and be useful in the development of target specific treatments.

Material and Methods

Experimental animals

All experiments were carried out in accordance with the Association for Research in Vision and Ophthalmology Statement for the use of Animals in Ophthalmic and Vision Research and were approved by the Institutional Animal Care and Use Committee of the University of Wisconsin School of Medicine and Public Health. We used a total of 12 albino female SD and 12 albino female Wistar rats (Harlan Sera-Laboratory; Indianapolis, IN). The rats were 12 weeks old at the start of the study and were kept in our vivarium under normal cyclic light (12 h on/off, 7 am-7 pm, Central Time) for a week prior to experimentation. The SD and Wistar rats were each divided into normal and intense cyclic light exposed groups. Both control and treated groups were further divided into three subgroups each. The three treated subgroups of SD and Wistar rats were exposed to 12 h of cyclic diffuse cool white 3,000 lux intensity light (36 watt compact fluorescent tubes, DL 930, Uplift Technologies, Dartmouth, Canada) for 1, 3, or 6 months, respectively. The corresponding three control subgroups were exposed to normal cyclic light used in the animal housing facility (~70 lux) for the same periods of time. The 12 h light/dark cycle was used to avoid alterations in the normal physiology of the rats by disturbing the circadian rhythms set by the eye.

In the treatment groups, pairs of clear plastic cages with wire tops were kept side by side with two light sources, one on each side of the two cages (i.e. one light source percage and two cages per shelf). Before placing rats inside respective cages and exposing them to light, light meter measurements (Fisher Scientific, Pittsburg, PA) were taken at the bottom of each cages to ensure equal light energy exposure inside the entire cage. The distance of the light sources, from either side of cages were adjusted to provide the desired reading. The control groups were kept in identical cages in a separate room under the normal cyclic vivarium lights. The light exposure of the control rats was measured in an identical manner to that of the treatment group. All rats were monitored for signs of abnormal behavior and appearance, and were weighed every other week for the duration of experiment.

Ocular evaluations

At the end of 1, 3, or 6 months, dilated fundoscopy, optical coherence tomography (OCT) and angiography procedures under anesthesia (intraperitoneal injection of 35 mg/kg ketamine hydrochloride and 5 mg/kg xylazine hydrochloride) were carried out. The pupils were dilated with 0.5% tropicamide and 2.5% phenylephrine hydrochloride eye drops. The topical endoscopy fundus imaging system was used to document changes in the retina following a technique previously described (31). Cirrus H D-OCT (Carl Zeiss Meditec, Germany) and Heidleberg retinal angiography system (HRA 2, Germany) were used to evaluate retinal edema and choroidal neovascularization using intraperitoneal injection of fluorescein sodium (60 mg/kg; Akron, Buffalo Grove, IL) and indocyanine green dye (6 mg/kg; Akron, Buffalo Grove, IL). The rat eyes were manually positioned in front of OCT and angiography camera to get the optimal view. The interpretation of OCT and angiography images were performed by two masked readers.

Histological evaluations

The rats were euthanized at respective time periods of 1, 3, or 6 months in a CO2 chamber. The eyes were enucleated and fixed in 10% neutral-buffered formalin. Further histological processing consisted of dehydration through increased concentration of alcohol, cleared with xylene, and embedded in a horizontal axis in paraffin. Six serial pupillary-optic nerve (PO) sections and four non-PO anterior-posterior sections of 8 μm thickness were obtained from each eye. These sections were stained with hematoxylin-eosin, periodic acid-Schiff, or Masson trichrome stain. Comparative histopathological evaluation of the neurosensory retina, RPE, Bruch's membrane, and choroid were performed in each eye by light microscopy. The retinal thickness was measured from internal limiting membrane to the outer limiting membrane. Measurements were taken at 4 corresponding areas (2 each on the nasal and temporal side of the optic disc). These areas were located at 0.5 mm and 1 mm away from the optic disc. The average retinal thickness was calculated for each treated and control rat after 1, 3, or 6 months of light exposure.

Immunofluorescence staining for oxidative stress related products

The extent of oxidative stress, in light exposed and control rats, was determined from the level of modifications of proteins by HNE and nitrotyrosine utilizing immunofluorescence staining of eye sections (32). Paraffin eye sections, prepared as described above, were washed in xylene 4 times (5 min each), and followed by two washes with 100% and 95% ethanol (10 min each), respectively. After two 5 min washes in water, sections were heated in microwave for 11 min for antigen retrieval (1600 ml of H_2O and 15 ml of vector H-3300; Vector Laboratories, Burlingame, CA) and allowed cool to room temperature overnight. Sections were then washed in water for 5 min, followed by three PBS washes (5 min each), and were incubated in blocker solution (1% BSA, 0.2% skim milk, and 0.3% Triton X-100 in PBS) for 15 min at room temperature. The blocked sections were then incubated with rabbit anti-4-Hydroxy-2-nonenal (HNE) antiserum (Alpha Diagnostic International, San Antonio, Texas), rabbit anti-nitrotyrosine (Invitrogen, Carlsbad, CA), rabbit-anti PCNA (Sigma, St. Louis, MO), rabbit-anti- Ki67 (DAKO, Carpentaria, CA), or rabbit IgG (Sigma; all prepared in blocking solution at 1:500 dilution) overnight at 4°C. After three washes with PBS (5 min each), sections were incubated with secondary antibody Alexa 594 goat-anti-rabbit (Invitrogen; 1:500 dilution prepared in blocking solution). Sections were washed three times with PBS, covered with PBS/glycerol (2 vol/1 vol), and mounted with a cover slip. Eye sections were viewed by fluorescence microscopy and images were captured in digital format using a Zeiss microscope (Carl Zeiss, Chester, VA).

Results

General health and ophthalmoscopic findings of animals

All treated and control groups of Wistar and SD rats appeared healthy after 1, 3, or 6 months of exposure to intense cyclic light. There were no observable changes in activity or eating and drinking habits in either group. In addition, no significant differences in the body weight of animals was observed at any point in the intense light exposed rats as compared to controls (not shown). Furthermore, on fundus examination, no obvious differences were noted in the appearance of the retinas between the control and treated groups in either the Wistar or SD rats. No retinal hemorrhage or exudative changes were noted in any animal.

Histology of Wistar rats

The comparative histological changes in Wistar and SD rats are summarized in Table 1. In control Wistar rats after 1 month of light exposure (Figures 1A, D), the inner and outer neurosensory layers, RPE, Bruch's membrane, and choroid were within normal limits, both in peripheral (Figure 1A) and central (Figure 1D) parts of retina. In contrast, the inner and outer segments were markedly atrophic and the thickness of ONL was reduced to less than one-third of the control Wistar rats after 1 month (Figure 1B). The effects were more severe in the central part of retina (Figure 1E). In a few central areas, swollen RPE cells with vacuolated cytoplasm were detached from Bruch's membrane (Figures 1F). The inner retinal layers were unremarkable in appearance. We did not observe migration of retinal capillaries toward the RPE layer at this time point.

After 3 months of light exposure, microscopic examinations of the control Wistar rats (Figure 2A) revealed normal morphology of the retinal layers and choroid. In the treated group (Figure 2B), there was almost total loss of the outer nuclear layer. We observed growth of new vessels extending from the choroid, penetrating Bruch's membrane, and invading the neurosensory retina. Migrating RPE cells encroached on the outer retinal layers, surrounding the new choroidal vessels (Figure 2C). We did not observe any retinal capillaries migrating towards RPE layer and RPE neovascularization. In addition, PCNA or Ki67 staining of sections from 1 month or 3 month intense cyclic light exposed rat showed no significant difference in RPE cell staining compared to control animals (not shown) indicating lack of increased RPE cell proliferation in intense light exposed animals.

After 6 months of light exposure, the RPE layer in the control groups was unremarkable with a normal anatomical arrangement of the overlying retinal layers (Figure 2D). In rats exposed to intense cyclic light, there was total loss of photoreceptor cells (Figure 2E). Additionally, the inner nuclear layer was thinned and contained many cells with pyknotic nuclei (Figures 2E, F). The newly formed choroidal vessels were anastomosed with retinal capillaries (Figure 2F), having an appearance similar to that described in late stages of various light or genetically induced rodent models of retinal degeneration (14). RPE cells migrated into the disorganized inner nuclear layer (Figure 3A). There was also fibrous metaplasia of the RPE, in which some of the cells had enlarged nuclei (Figure 3B). Extracellular deposits (Figure 3C) were also present and the RPE layer was thickened, basophilic, and contained microcystoid spaces (Figure 3D). The extracellular deposits were stained positive with PAS stain (Figure 3E). Fibrovascular tissues were extended between the choroid and the inner retinal capillary layer adhering the choroid to the retina (Figure 3F).

Staining for oxidative products

One of the most damaging effects of ROS production is initiation of lipid peroxidation, a radical chain reaction when ROS oxidize cellular membrane lipids. 4-hydroxy-2-nonenal (HNE), one of the major aldehydic products of the peroxidation of membrane ω-6 polyunsaturated fatty

acids provides a measure of this process and can also contribute to oxidant stress mediated cell injury (33). The staining for HNE-modified proteins was more prominent in the intense light exposed Wistar rats compared to the corresponding control groups (Figures 4A, B). HNE staining was more concentrated in ganglion cells, inner, and outer nuclear layers compared to inner and outer plexiform layers. The staining for nitrotyrosine-modified proteins, a byproduct of peroxynitrite generated from nitric oxide synthase uncoupling under oxidative stress (34), was more prominent in intense light exposed Wistar rats compared to control (Figures 4C, D). No staining was observed using control rabbit IgG (not shown).

Histology of Sprague-Dawley rats

The intense cyclic light exposed SD rate exhibited similar pathological changes in the retina, Bruch's membrane, and choroid as those described in Wistar rats (Figure 5). However, these changes developed more slowly and were less severe in the light exposed SD rats compared to Wistar rats (Table I). The foci of sub-RPE neovascularization were first evident after 3 months of light exposure in the SD rats compared to Wistar rats, which was present after 1 month of light exposure. Retinal thickness measurements and immunostaining results (HNE and nitrotyrosine) were similar to those observed in Wistar rats (not shown). In addition, no RPE neovascularization arising from the retinal capillaries was observed at the time points studied (Figure 5).

Optical Coherence Tomography

In both treated Wistar and SD rats, areas of higher reflectivity were seen extending through the normal retina from the RPE and choroid in the 6-month intense light-exposed rats that were not present in the control unexposed groups (Figure 6). The retina was thinned with loss of inner and outer segments of photoreceptors. The RPE interface in the light exposed group showed more irregularity in the light-treated animals than in the control groups. There were hyporeflective areas within the retina suggestive of leakage of fluid from microvasculature of CNV in the treated groups (Figure 6B). The presence of fluid signifies that the proliferating vessels are leaky and, thus, abnormally forming, as occurs in humans with exudative AMD. These changes were less marked after 1 or 3 months of light exposure (not shown). The retinal thickness measurements are shown in Figure 6C. The average retinal thickness in light exposed Wistar rats was reduced to about 90 micron after 1 month, 70 micron after 3 months, and 50 micron after 6 months. In contrast, the average retinal thickness in the control groups remained stable at 140 micron after 1, 3, or 6 months.

Indocyanine green and fluorescein angiography

After 6 months of intense light exposure, ICG angiography in the Wister rats showed early peripapillary hyperfluorescence that increased in a late phase, suggestive of prominent CNV (Figures 7A, B). Fluorescein angiography (Figures 7C, D) demonstrated multiple areas of CNV with hyperfluorescence suggestive of surrounding leakage. Additionally, hypoperfused areas invaded by leaking new retinal vessels were also observed. In contrast, the control group did not show any foci of neovascularization or leakage on either ICG (Figure 7E) or fluorescein angiography (Figure 7F).

The leakage of dye from the new vessels is suggestive of their prematurity and thus pathological neovascularization. The fluorescein angiography showed intraretinal neovascular networks and marked leakage from the proliferating new retinal vessels. The peripapillary choroidal neovascularization was more prominently observed in ICG angiography. ICG dye can delineate choroidal vasculature better than fluorescein dye (35). These leakage foci are representing the histologically seen proliferating new choroidal vessels encroaching on the overlying retinal layers. Choroidal neovascular membranes often are poorly defined on fluorescein angiography because of rapid or indistinct fluorescein leakage or because of blockage of hyperfluorescence

by overlying hemorrhage, lipid, turbid fluid, or pigment. Compared with fluorescein angiography, ICG improved visualization of the choroidal circulation and enhanced visualization of some membranes that were poorly defined with fluorescein. A similar result was noted in the SD rats (not shown).

Discussion

This study demonstrates the progressive stages of intense cyclic light induced retinal degeneration in albino Wistar and SD rats. The pathologic process progressed from 1) an early stage of photoreceptor loss, partial outer nuclear layer loss, and alteration in the RPE layer to 2) total loss of outer nuclear layer and partial loss of inner nuclear layer to 3) sub-RPE neovascularization, disruption of Bruch's membrane, and finally anastomosis of newly formed choroidal vessels with retinal capillaries in the outer retina. This study demonstrates the progression to an advanced stage that to the best of our knowledge has not been previously described. These progressive pathologic changes simulate the growth patterns of human CNV as described by Grossniklaus and Green (36). These investigators observed on histological examination three patterns of new vessel formation: sub-RPE, sub-retinal, and combined growth. Furthermore, the features described here are also similar to the published histological reports of human cadaver eyes with CNV (37–43). Thus, we believe that the intense cyclic light-induced CNV model described in this study closely resembles the progressive human pathology, and accordingly may be a useful model for study and treatment of human exudative AMD.

The development of neovascularization is a critical component of the pathogenesis of human exudative AMD resulting in visual loss. If left untreated, these new vessels result in intraretinal and/or subretinal hemorrhages and exudates, leading to destruction of viable retinal cells (44). The inhibition of CNV and new vessel growth within the retina by VEGF antagonists has been an important milestone in the treatment of exudative AMD in patients (45). However, significant improvement of vision is only observed in 30% of the patients and, 20% of the patients had a decrease in visual acuity resulting in legal blindness (45). In addition, potential systemic ill effects following continuous inhibition of VEGF at sites necessary for normal functions, such as retina (46,47) and renal glomeruli (48), is of increasing concern. Thus, the development of additional treatment strategies with a more specific targeting of the pathologies associated with exudative AMD is desirable.

Various animal models have been instrumental in advancing our understanding of both the pathogenesis of AMD and the development and testing of effective treatments for AMD (49). An early and important animal model was the laser induced CNV, developed by Ryan et al. in 1979 (50) and it remains one of the commonly used models for exudative AMD research. This was followed by numerous transgenic models and surgically injected growth factor induced CNV models. A comparison of the model described here with other major CNV models is presented in Table 2. Among the available transgenic models, $Ccl2^{-/-}$ and $Ccr2^{-/-}$ deficient models (51), VLDLR mouse strain (52,53), hephaestin and ceruloplasmin double-knockout mice model (54), and Sod1-deficient mice (55) showed development of CNV. However, these pathologic changes were only observed in significantly older animals, 10–15 months of age. In addition, the corresponding genes causing the retinal changes in these models have not been associated directly with AMD in humans (56). Thus, availability of models that develop the entire spectrum of AMD associated pathologic changes within a reasonably short duration would be extremely useful in the study of the disease and the development and testing of new target specific treatments.

Oxidative stress is one of the pathological processes recognized to be involved in human AMD (21,57,58). The increased oxidative stress induced byproducts, HNE and nitrotyrosine, in the

degenerated retina with light-induced CNV were observed in our model, as previously reported in light-exposed rat retina (59). Among models using light as the stimulus, Cousin et al. (60) reported the presence of basal laminar deposits with excessive fatty diets that increased in severity with brief exposure to blue light. In contrast, the rats in our study were fed a normal diet but exposed to prolonged duration of 3000 lux intensity cyclic white light and developed sub-RPE deposition of amorphous material similar to basal laminar deposits described in the literature (61).

A focal photic injury had been used to stimulate CNV in the past but never in association with retinal degeneration related to light exposure (62). Although neovascularization has been previously reported in various animal models of retinal degeneration, the majority of these have an origin from retinal capillaries and extended to the RPE and choroid resulting in RPE neovascularization (13,14). The RPE cells survive the light exposure and for the most part remain unchanged, except for compaction of the villous processes in the retinal zone where the photoreceptors resided prior to their destruction. We did not observe changes in retinal capillaries of animals exposed to intense cyclic light, at one and three months of treatment.

Unfortunately, in the majority of early studies of light-induced retinal degeneration models, the temporal changes were not carefully evaluated in terms of the site of initiation and the manner of progression of neovascularization. However, detailed temporal evaluation of the loss of photoreceptors and retinal vasculature in rhodopsin transgenic rats recently demonstrated a direct relationship between loss of 18 photoreceptor cells and attenuation of normal retinal vascularization during early stages of retinal vascular development (14). The rapid loss of photoreceptor cells in younger animals had its most severe impact on inner retinal vascularization, and over time did not show RPE neovascularization arising from retinal capillaries. The impact on the RPE cells was also minimal in these animals. These observations are consistent with those reported in the present study in rats exposed to intense cyclic light, where extensive loss of photoreceptor cells was observed by the first month. This was concomitant with the migration of newly formed choroidal- not retinal- blood vessels growing toward the outer retina. The RPE cells appeared, for the most part, within normal limits at 1 and 3 month of intense light exposure, with minimal sign of proliferation determined by PCNA or Ki67 staining (not shown). However, loss of RPE polarization and organization of RPE cells around the newly forming choroidal blood vessels were observed. Thus, our results suggest that the rapid loss of photoreceptor cells may promote the formation of new choroidal vessels in order to accommodate the oxygen need of outer retina.

Neovascularization of the RPE by retinal capillaries is a common feature of inherited and environmentally induced retinal degeneration in rodents (13,14,63,64). However, vascularization of the RPE is not known to occur in human diseases of photoreceptor degeneration, such as retinitis pigmentosa (65). Although it is suggested that other types of neovascularization may occur, their source and pathogenesis remain elusive. Furthermore, the studies in different rodent models of retinal degeneration suggest a major contributing factor may be temporal (i.e. the rate at which photoreceptors degenerate) and thus determines the involvement of retinal or choroidal capillaries as the source of vascularization of outer retina. Thus, the gradual loss of photoreceptor cells over time may favor migration of retinal capillaries with consequent RPE neovascularization. The molecular and cellular mechanisms which discriminate between these pathways remain elusive and need further study.

In summary, our rat model displayed progressive stages of retinal degeneration, with features of newly forming choroidal vessels closely resembling that seen in human exudative AMD, induced by chronic intense cyclic light exposure within a relatively short time. We believe the chronic intense cyclic light-induced exudative AMD model described here will prove useful

in, not only the evaluation of molecular and cellular mechanisms associated with exudative AMD but, also for effective screening of new compounds with potential therapeutic potential.

Acknowledgments

This work was supported in part by grants EY16995 and EY18179 (NS), and P30 EY16665 from the National Institutes of Health, and an unrestricted departmental award from Research to Prevent Blindness. NS is a recipient of a Research Award from Retina Research Foundation. We thank Dr. Jaal B. Ghandhi from the School of Engineering for assistant with the design and measurement of the intense cyclic lighting. We also thank Elizabeth A. Scheef for preparation of figures and Carol Rasmussen for help with OCT ICG, and fluorescein angiography.

References

1. Ambati J, Ambati BK, Yoo SH, Ianchulev S, Adamis AP. Age-related macular degeneration: etiology, pathogenesis, and therapeutic strategies. Surv Ophthalmol 2003;48:257–293. [PubMed: 12745003]
2. Ding X, Patel M, Chan CC. Molecular pathology of age-related macular degeneration. Prog Retin Eye Res 2009;28:1–18. [PubMed: 19026761]
3. Jager RD, Mieler WF, Miller JW. Age-Related Macular Degeneration. N Engl J Med 2008;358:2606–2617. [PubMed: 18550876]
4. Jager RD, Mieler WF, Miller JW. Age-related macular degeneration. N Engl J Med 2008;358:2606–2617. [PubMed: 18550876]
5. McLeod DS, Grebe R, Bhutto I, Merges C, Baba T, Lutty GA. Relationship between RPE and Choriocapillaris in Age-Related Macular Degeneration. Invest Ophthalmol Vis Sci 2009;50:4982–4991. [PubMed: 19357355]
6. Elizabeth Rakoczy P, Yu MJT, Nusinowitz S, Chang B, Heckenlively JR. Mouse models of age-related macular degeneration. Exp Eye Res 2006;82:741–752. [PubMed: 16325179]
7. Green WR. Histopathology of age-related macular degeneration. Mol Vis 1999;5:27. [PubMed: 10562651]
8. Campochiaro PA, Soloway P, Ryan SJ, Miller JW. The pathogenesis of choroidal neovascularization in patients with age-related macular degeneration. Mol Vis 1999;5:34. [PubMed: 10562658]
9. Cruickshanks KJ, Klein R, Klein BE. Sunlight and age-related macular degeneration. The Beaver Dam Eye Study. Arch Ophthalmol 1993;111:514–518. [PubMed: 8470986]
10. Noell WK, Walker VS, Kang BS, Berman S. Retinal damage by light in rats. Invest Ophthalmol 1966;5:450–473. [PubMed: 5929286]
11. Kuwabara T, Gorn RA. Retinal damage by visible light. An electron microscopic study. Arch Ophthalmol 1968;79:69–78. [PubMed: 5635094]
12. O'Steen WK, Shear CR, Anderson KV. Retinal damage after prolonged exposure to visible light. A light and electron microscopic study. Am J Anat 1972;134:5–21. [PubMed: 5031977]
13. Burns MS, Tyler NK. Selective neovascularization of the retinal pigment epithelium in rat photoreceptor degeneration in vivo. Curr Eye Res 1990;9:1061–1075. [PubMed: 1710178]
14. Nishikawa S, LaVail MM. Neovascularization of the RPE: temporal differences in mice with rod photoreceptor gene defects. Exp Eye Res 1998;67:509–515. [PubMed: 9878212]
15. Pennesi ME, Nishikawa S, Matthes MT, Yasumura D, LaVail MM. The relationship of photoreceptor degeneration to retinal vascular development and loss in mutant rhodopsin transgenic and RCS rats. Exp Eye Res 2008;87:561–570. [PubMed: 18848932]
16. Kremers JJM, van Norren D. Two classes of photochemical damage of the retina. Lasers Light Ophthalmol 1988;2:41–52.
17. O'Steen WK, Anderson KV. Photoreceptor degeneration after exposure of rats to incandescent illumination. Z Zellforsch Mikrosk Anat 1972;127:306–313. [PubMed: 5029819]
18. O'Steen WK, Anderson KV, Shear CR. Photoreceptor degeneration in albino rats: dependency on age. Invest Ophthalmol 1974;13:334–339. [PubMed: 4823176]
19. Lanum J. The damaging effects of light on the retina. Empirical findings, theoretical and practical implications. Surv Ophthalmol 1978;22:221–249. [PubMed: 416513]

20. Wiegand RD, Giusto NM, Rapp LM, Anderson RE. Evidence for rod outer segment lipid peroxidation following constant illumination of the rat retina. Invest Ophthalmol Vis Sci 1983;24:1433–1435. [PubMed: 6618806]
21. Hollyfield JG, Bonilha VL, Rayborn ME, et al. Oxidative damage-induced inflammation initiates age-related macular degeneration. Nat Med 2008;14:194–198. [PubMed: 18223656]
22. Demontis GC, Longoni B, Marchiafava PL. Molecular steps involved in light-induced oxidative damage to retinal rods. Invest Ophthalmol Vis Sci 2002;43:2421–2427. [PubMed: 12091446]
23. Wu J, Seregard S, Algvere PV. Photochemical damage of the retina. Surv Ophthalmol 2006;51:461–481. [PubMed: 16950247]
24. Donovan M, Carmody RJ, Cotter TG. Light-induced photoreceptor apoptosis in vivo requires neuronal nitric-oxide synthase and guanylate cyclase activity and is caspase-3-independent. J Biol Chem 2001;276:23000–23008. [PubMed: 11278285]
25. Wu J, Gorman A, Zhou X, Sandra C, Chen E. Involvement of caspase-3 in photoreceptor cell apoptosis induced by in vivo blue light exposure. Invest Ophthalmol Vis Sci 2002;43:3349–3354. [PubMed: 12356844]
26. Dong A, Xie B, Shen J, et al. Oxidative stress promotes ocular neovascularization. J Cell Physiol 2009;219:544–552. [PubMed: 19142872]
27. Weale RA. Do years or quanta age the retina? Photochem Photobiol 1989;50:429–438. [PubMed: 2675140]
28. Age-Related Eye Disease Study Research G. A Randomized, Placebo-Controlled, Clinical Trial of High-Dose Supplementation With Vitamins C and E, Beta Carotene, and Zinc for Age-Related Macular Degeneration and Vision Loss: AREDS Report No. 8. Arch Ophthalmol 2001;119:1417–1436. [PubMed: 11594942]
29. Dianzani MU, Barrera G, Parola M. 4-Hydroxy-2,3-nonenal as a signal for cell function and differentiation, Acta Biochim. Pol 1999;46:61–75.
30. Miyagi M, Sakaguchi H, Darrow RM, et al. Evidence that light modulates protein nitration in rat retina. Mol Cell Proteomics 2002;1:293–303. [PubMed: 12096111]
31. Paques M, Guyomard JL, Simonutti M, et al. Panretinal, high-resolution color photography of the mouse fundus. Invest Ophthalmol Vis Sci 2007;48:2769–2774. [PubMed: 17525211]
32. Tang Y, Scheef EA, Wang S, et al. CYP1B1 expression promotes the proangiogenic phenotype of endothelium through decreased intracellular oxidative stress and thrombospondin-2 expression. Blood 2009;113:744–754. [PubMed: 19005183]
33. Esterbauer H, Schaur RJ, Zollner H. Chemistry and biochemistry of 4-hydroxynonenal, malonaldehyde and related aldehydes. Free Radic Biol Med 1991;11:81–128. [PubMed: 1937131]
34. Platt DH, Bartoli M, El-Remessy AB, et al. Peroxynitrite increases VEGF expression in vascular endothelial cells via STAT3. Free Radic Biol Med 2005;39:1353–1361. [PubMed: 16257644]
35. Destro M, Puliafito CA. Indocyanine green videoangiography of choroidal neovascularization. Ophthalmology 1989;96:846–853. [PubMed: 2472588]
36. Grossniklaus HE, Green WR. Choroidal neovascularization. Am J Ophthalmol 2004;137:496–503. [PubMed: 15013874]
37. Sarks SH. New vessel formation beneath the retinal pigment epithelium in senile eyes. Br J Ophthalmol 1973;57:951–965. [PubMed: 4788954]
38. D'Amore PA. Mechanisms of retinal and choroidal neovascularization. Invest Ophthalmol Vis Sci 1994;35:3974–3979. [PubMed: 7525506]
39. Small ML, Green WR, Alpar JJ, Drewry RE. Senile mecular degeneration. A clinicopathologic correlation of two cases with neovascularization beneath the retinal pigment epithelium. Arch Ophthalmol 1976;94:601–607. [PubMed: 1267640]
40. Lopez PF, Grossniklaus HE, Lambert HM, et al. Pathologic features of surgically excised subretinal neovascular membranes in age-related macular degeneration. Am J Ophthalmol 1991;112:647–656. [PubMed: 1957899]
41. Castellarin AA, Nasir MA, Sugino IK, Zarbin MA. Clinicopathological correlation of primary and recurrent choroidal neovascularisation following surgical excision in age related macular degeneration. Br J Ophthalmol 1998;82:480–487. [PubMed: 9713052]

42. Grossniklaus HE, Hutchinson AK, Capone A Jr, Woolfson J, Lambert HM. Clinicopathologic features of surgically excised choroidal neovascular membranes. Ophthalmology 1994;101:1099–1111. [PubMed: 7516516]
43. Lambert HM, Capone A Jr, Aaberg TM, Sternberg P Jr, Mandell BA, Lopez PF. Surgical excision of subfoveal neovascular membranes in age-related macular degeneration. Am J Ophthalmol 1992;113:257–262. [PubMed: 1371906]
44. Ferris FL 3rd, Fine SL, Hyman L. Age-related macular degeneration and blindness due to neovascular maculopathy. Arch Ophthalmol 1984;102:1640–1642. [PubMed: 6208888]
45. Rosenfeld PJ, Rich RM, Lalwani GA. Ranibizumab: Phase III clinical trial results. Ophthalmol Clin North Am 2006;19:361–372. [PubMed: 16935211]
46. Famiglietti EV, Stopa EG, McGookin ED, Song P, LeBlanc V, Streeten BW. Immunocytochemical localization of vascular endothelial growth factor in neurons and glial cells of human retina. Brain Res 2003;969:195–204. [PubMed: 12676380]
47. Nishijima K, Ng YS, Zhong L, et al. Vascular endothelial growth factor-A is a survival factor for retinal neurons and a critical neuroprotectant during the adaptive response to ischemic injury. Am J Pathol 2007;171:53–67. [PubMed: 17591953]
48. Eremina V, Jefferson JA, Kowalewska J, et al. VEGF inhibition and renal thrombotic microangiopathy. N Engl J Med 2008;358:1129–1136. [PubMed: 18337603]
49. Evans J, Wormald R. Is the incidence of registrable age-related macular degeneration increasing? Br J Ophthalmol 1996;80:9–14. [PubMed: 8664242]
50. Ryan SJ. The development of an experimental model of subretinal neovascularization in disciform macular degeneration. Trans Am Ophthalmol Soc 1979;77:707–745. [PubMed: 94717]
51. Ambati J, Anand A, Fernandez S, et al. An animal model of age-related macular degeneration in senescent Ccl-2- or Ccr-2-deficient mice. Nat Med 2003;9:1390–1397. [PubMed: 14566334]
52. Frykman PK, Brown MS, Yamamoto T, Goldstein JL, Herz J. Normal plasma lipoproteins and fertility in gene-targeted mice homozygous for a disruption in the gene encoding very low density lipoprotein receptor. Proc Natl Acad Sci U S A 1995;92:8453–8457. [PubMed: 7667310]
53. Heckenlively JR, Chang B, Erway LC, et al. Mouse model for Usher syndrome: linkage mapping suggests homology to Usher type I reported at human chromosome 11p15. Proc Natl Acad Sci U S A 1995;92:11100–11104. [PubMed: 7479945]
54. Hahn P, Qian Y, Dentchev T, et al. Disruption of ceruloplasmin and hephaestin in mice causes retinal iron overload and retinal degeneration with features of age-related macular degeneration. Proc Natl Acad Sci U S A 2004;101:13850–13855. [PubMed: 15365174]
55. Imamura Y, Noda S, Hashizume K, et al. Drusen, choroidal neovascularization, and retinal pigment epithelium dysfunction in SOD1-deficient mice: A model of age-related macular degeneration. Proceedings of the National Academy of Sciences 2006;103:11282–11287.
56. Marmorstein AD, Marmorstein LY. The challenge of modeling macular degeneration in mice. Trends Genet 2007;23:225–231. [PubMed: 17368622]
57. Winkler BS, Boulton ME, Gottsch JD, Sternberg P. Oxidative damage and age-related macular degeneration. Mol Vis 1999;5:32. [PubMed: 10562656]
58. Beatty S, Koh H, Phil M, Henson D, Boulton M. The role of oxidative stress in the pathogenesis of age-related macular degeneration. Surv Ophthalmol 2000;45:115–134. [PubMed: 11033038]
59. Tanito M, Elliott MH, Kotake Y, Anderson RE. Protein modifications by 4-hydroxynonenal and 4-hydroxyhexenal in light-exposed rat retina. Invest Ophthalmol Vis Sci 2005;46:3859–3868. [PubMed: 16186375]
60. Cousins SW, Espinosa-Heidmann DG, Alexandridou A, Sall J, Dubovy S, Csaky K. The role of aging, high fat diet and blue light exposure in an experimental mouse model for basal laminar deposit formation. Exp Eye Res 2002;75:543–553. [PubMed: 12457866]
61. Curcio CA, Presley JB, Millican CL, Medeiros NE. Basal deposits and drusen in eyes with age-related maculopathy: evidence for solid lipid particles. Exp Eye Res 2005;80:761–775. [PubMed: 15939032]
62. Heriot WJ, Henkind P, Bellhorn RW, Burns MS. Choroidal neovascularization can digest Bruch's membrane. A prior break is not essential. Ophthalmology 1984;91:1603–1608. [PubMed: 6084226]

63. Caldwell RB, Roque RS, Solomon SW. Increased vascular density and vitreo-retinal membranes accompany vascularization of the pigment epithelium in the dystrophic rat retina. Curr Eye Res 1989;8:923–937. [PubMed: 2477196]
64. Weber ML, Mancini MA, Frank RN. Retinovitreal neovascularization in the Royal College of Surgeons rat. Curr Eye Res 1989;8:61–74. [PubMed: 2468452]
65. Uliss AE, Gregor ZJ, Bird AC. Retinitis pigmentosa and retinal neovascularization. Ophthalmology 1986;93:1599–1603. [PubMed: 2433659]
66. Lu B, Rutledge BJ, Gu L, et al. Abnormalities in monocyte recruitment and cytokine expression in monocyte chemoattractant protein 1-deficient mice. J Exp Med 1998;187:601–608. [PubMed: 9463410]
67. Kuziel WA, Morgan SJ, Dawson TC, et al. Severe reduction in leukocyte adhesion and monocyte extravasation in mice deficient in CC chemokine receptor 2. Proc Natl Acad Sci U S A 1997;94:12053–12058. [PubMed: 9342361]
68. Ohno-Matsui K, Hirose A, Yamamoto S, et al. Inducible expression of vascular endothelial growth factor in adult mice causes severe proliferative retinopathy and retinal detachment. Am J Pathol 2002;160:711–719. [PubMed: 11839592]
69. Obata H, Kaburaki T, Kato M, Yamashita H. Expression of TGF-beta type I and type II receptors in rat eyes. Curr Eye Res 1996;15:335–340. [PubMed: 8654115]
70. Schwesinger C, Yee C, Rohan RM, et al. Intrachoroidal neovascularization in transgenic mice overexpressing vascular endothelial growth factor in the retinal pigment epithelium. Am J Pathol 2001;158:1161–1172. [PubMed: 11238064]
71. Heckenlively JR, Hawes NL, Friedlander M, et al. Mouse model of subretinal neovascularization with choroidal anastomosis. Retina 2003;23:518–522. [PubMed: 12972764]
72. Shen D, Wen R, Tuo J, Bojanowski CM, Chan CC. Exacerbation of retinal degeneration and choroidal neovascularization induced by subretinal injection of Matrigel in CCL2/MCP-1-deficient mice. Ophthalmic Res 2006;38:71–73. [PubMed: 16352919]
73. Zhao L, Wang Z, Liu Y, et al. Translocation of the retinal pigment epithelium and formation of sub-retinal pigment epithelium deposit induced by subretinal deposit. Mol Vis 2007;13:873–880. [PubMed: 17615538]
74. Kimura H, Sakamoto T, Hinton DR, et al. A new model of subretinal neovascularization in the rabbit. Invest Ophthalmol Vis Sci 1995;36:2110–2119. [PubMed: 7657549]
75. Ozaki H, Hayashi H, Vinores SA, Moromizato Y, Campochiaro PA, Oshima K. Intravitreal sustained release of VEGF causes retinal neovascularization in rabbits and breakdown of the blood-retinal barrier in rabbits and primates. Exp Eye Res 1997;64:505–517. [PubMed: 9227268]

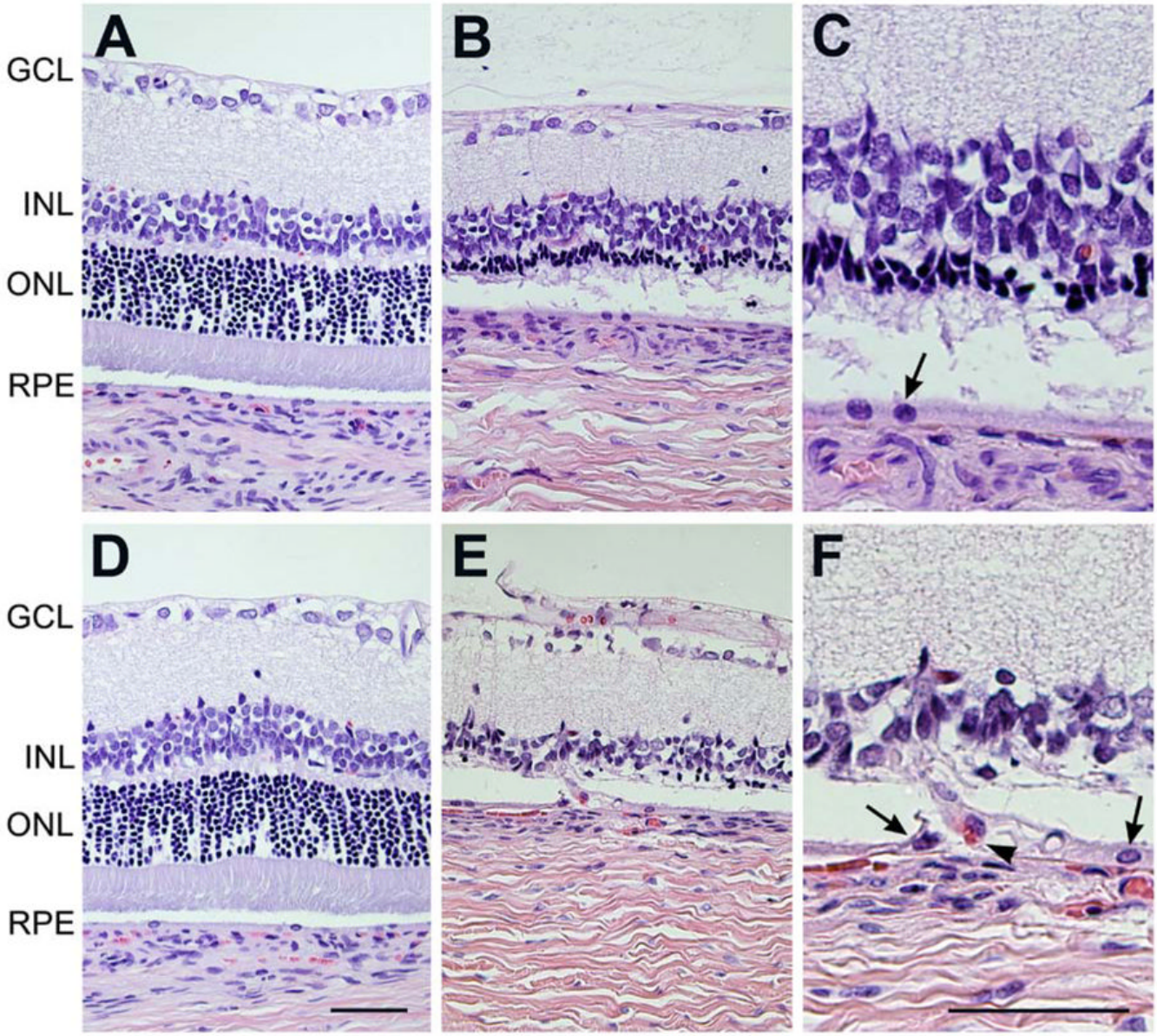

Figure 1.

Histological evaluation of Wistar rats after 1 month of intense cyclic light exposure. Comparable H&E stained sections of retina of control (A, D) rats vs. intense light exposed rats (B, C, E, F), from peripheral (A–C) and central (D–F) parts of retina were evaluated. The appearance of retinas was within normal limits in control Wistar rats at both peripheral (A) and central (D) part of the retina. The outer nuclear layer was reduced from 1/3 of its full thickness to total absence in intense cyclic light exposed Wistar rats (B, E). The layers of photoreceptor inner and outer segments were completely degenerated after 1 month of intense light exposure (E, F). Please note that the central part of the retina (E, F) is more affected in intense cyclic light exposed rats than the periphery (B, C). C and F are higher magnifications (x400) of B and E (x200). Arrow show RPE cells and arrow heads show red blood cell. Representative images are shown. All animals exposed to intense cyclic light exhibited a similar phenotype. GCL: ganglion cell layer; INL: inner nuclear layer; ONL: outer nuclear layer; RPE: retinal pigment epithelium. Bar= 50 μm.

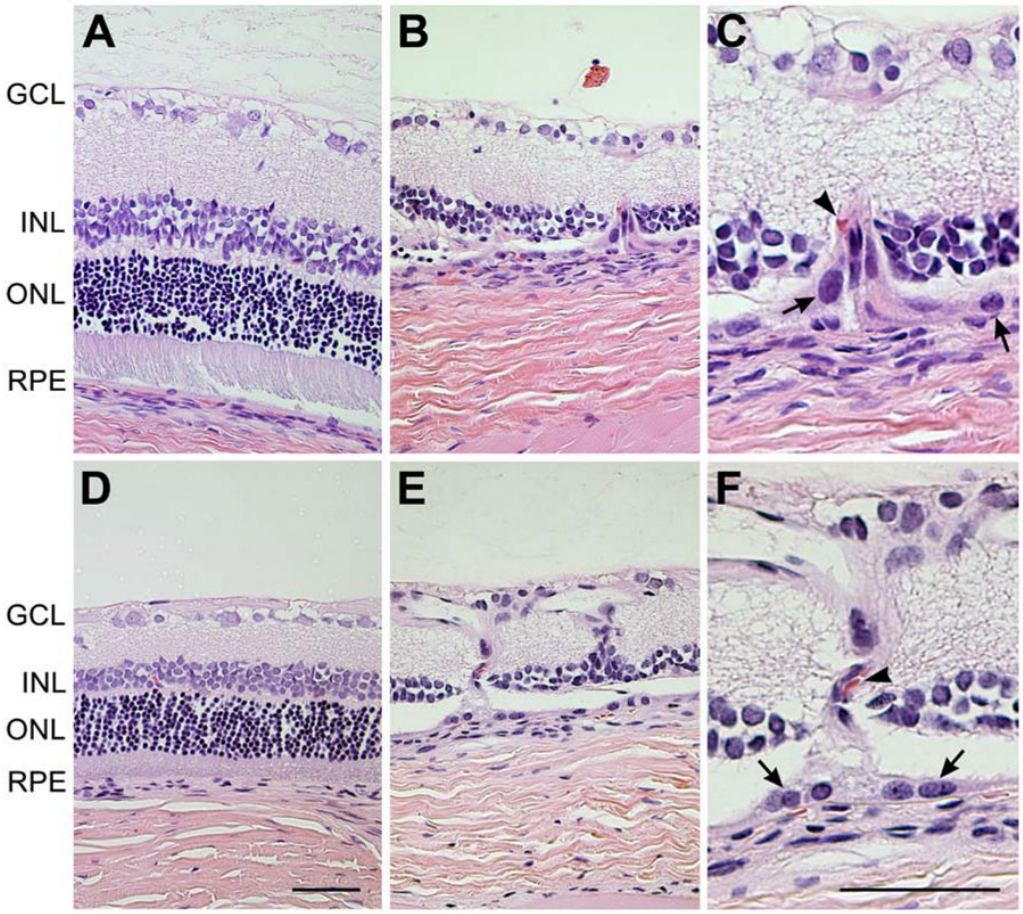

Figure 2.

Histological evaluation of Wistar rats after 3 or 6 month of intense cyclic light exposure. Comparable H&E stained sections of retina of control (A, D) rats vs. intense light exposed rats (B, C, E, F), from central parts of retina were evaluated. All layers of the retina were intact in control Wistar rat after 3 months (A). In intense light exposed rats, the inner and outer segments and outer nuclear layer was completely absent and a part of the inner nuclear layer was also affected (B). Areas of sub-RPE vascularization extending into the overlying degenerated retina were frequently observed after 3 months of intense light exposure (C). After 6 months of intense light exposure, the retina was within normal limits in the control Wistar rat group (D). Multiple areas of choroidal neovascularization with fibrotic bands anastomosing with the retinal capillary layer were observed in intense light exposed rats after 6 months (E, F). C and F are higher magnifications (x400) of B and E (x200). Arrows show RPE cells and arrow heads show red blood cells. Representative images are shown. All animals exposed to intense cyclic light exhibited a similar phenotype. GCL: ganglion cell layer; INL: inner nuclear layer; ONL: outer nuclear layer; RPE: retinal pigment epithelium. Bar=50 μm.

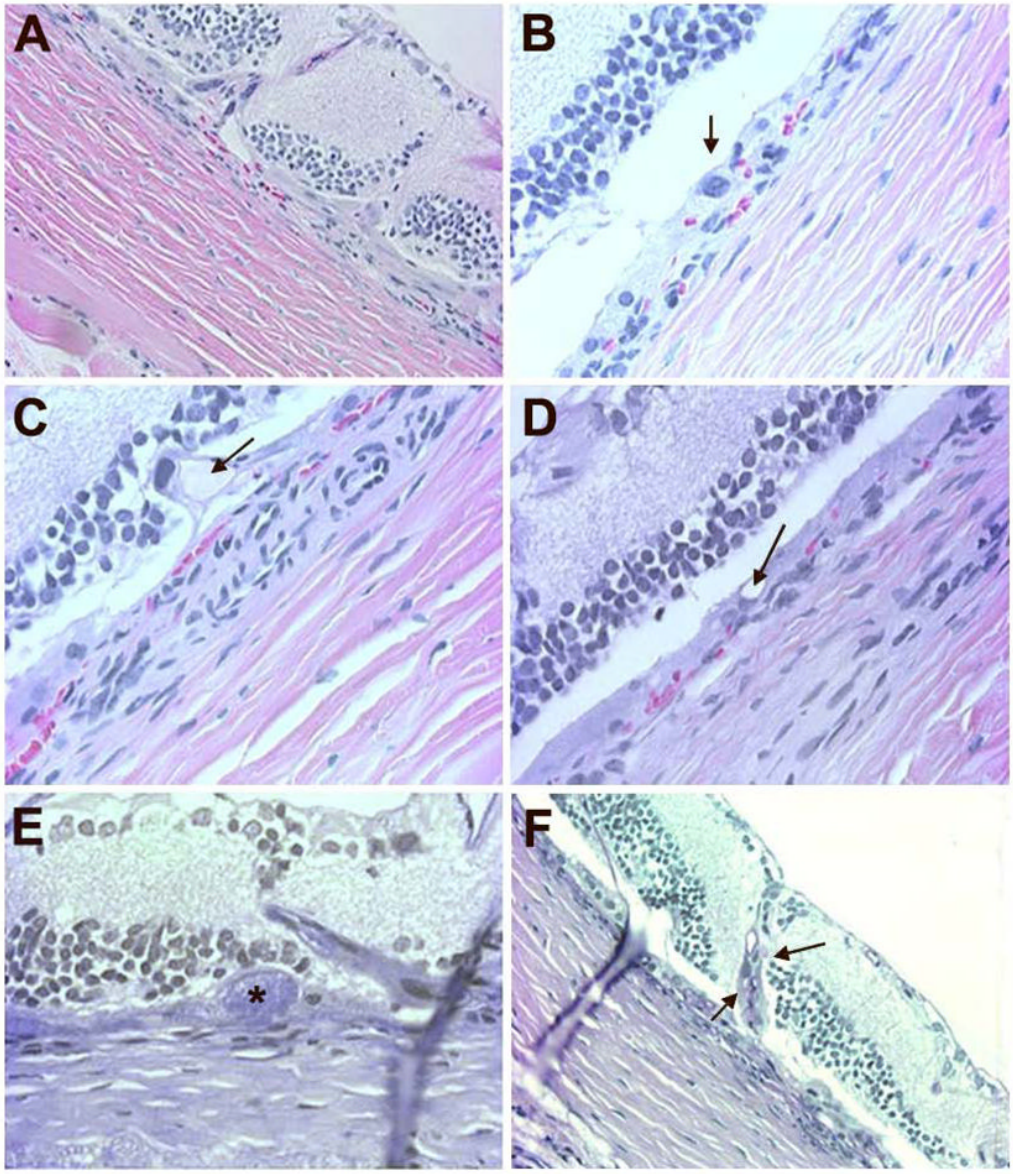

Figure 3.

Histological evaluation of Wistar rats after 6 months of intense cyclic light exposure. H & E (A, B, C, D) and PAS (E, F) stained sections of the retina from intense light exposed Wistar rats were evaluated. Migrating RPE cells and disorganized inner nuclear layer with new vessels growing towards ganglion cells is shown (A). Thickened RPE layer with an enlarged RPE nucleus and abundant cytoplasm is shown (B). A proteinaceous deposit (arrow) along RPE cell layer and Bruch's membrane was present (C). Basophilic RPE-Bruch's membrane complex with microcystoid spaces (arrow) were also present (D). PAS positive deposit (*) along RPE layer is shown (E). A blood vessel growing from choroid into the retina (arrows) stained positive on PAS was visible (F). Representative images are shown. All animals exposed to light exhibited a similar phenotype.

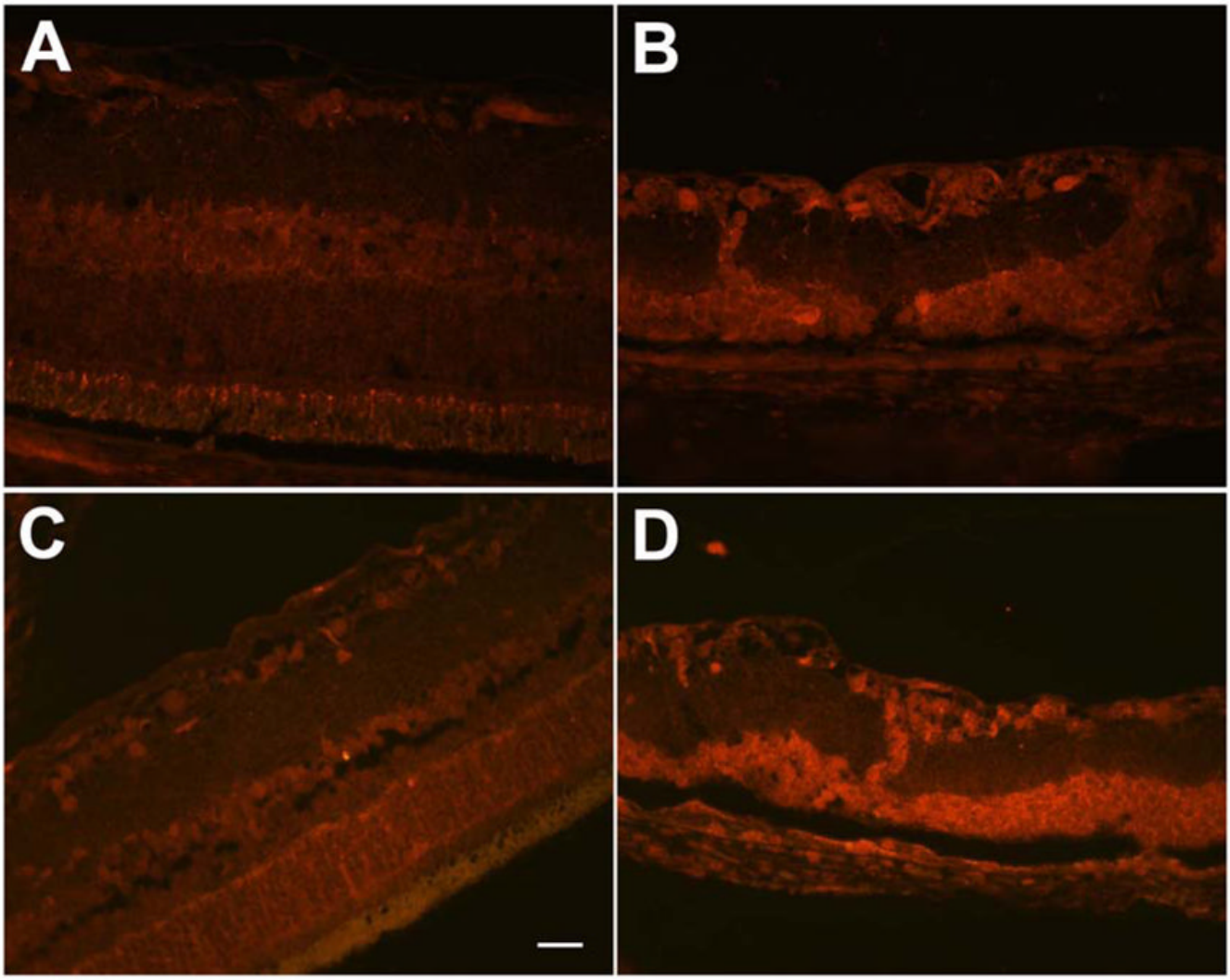

Figure 4.

Increased oxidative stress in Wistar rats exposed to intense cyclic light. The retina of control Wistar rat (A) showed less staining for HNE (4-hydroxy-2-nonenal)-modified proteins compared to intense light exposed Wistar rat (B). Similarly nitrotyrosine staining was much less prominent in the control Wistar rat (C) compared to intense light exposed Wistar rat (D). The retina of the light exposed rats (B, D) was thinner and degenerated compared to control rats (A, C), due to light induced degenerative changes in the outer retinal layers. No staining was observed in slides incubated with rabbit IgG (not shown). Bar= 50 μm.

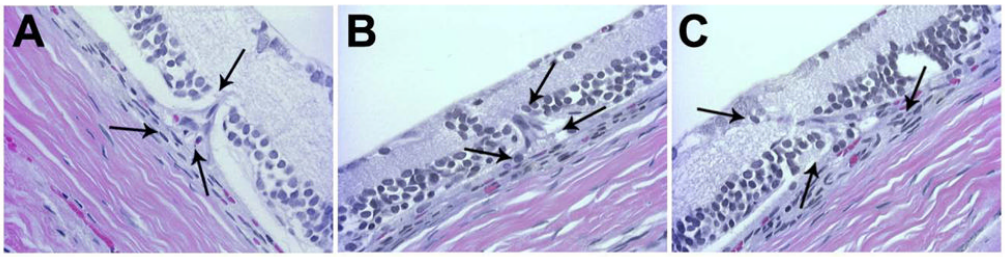

Figure 5.
Histological evaluation of Sprague-Dawley rats after 6 months of intense cyclic light exposure. Three progressive stages of CNV formation were observed. A focal sub-RPE neovascularization with an intact Bruch's membrane (A), disruption of Bruch's membrane (B) and invasion of CNV into the degenerated retina (C) is demonstrated. Arrows are indicating the growing CNV affected area of the degenerated retina. Representative images are shown. All animals exposed to light exhibited a similar phenotype.

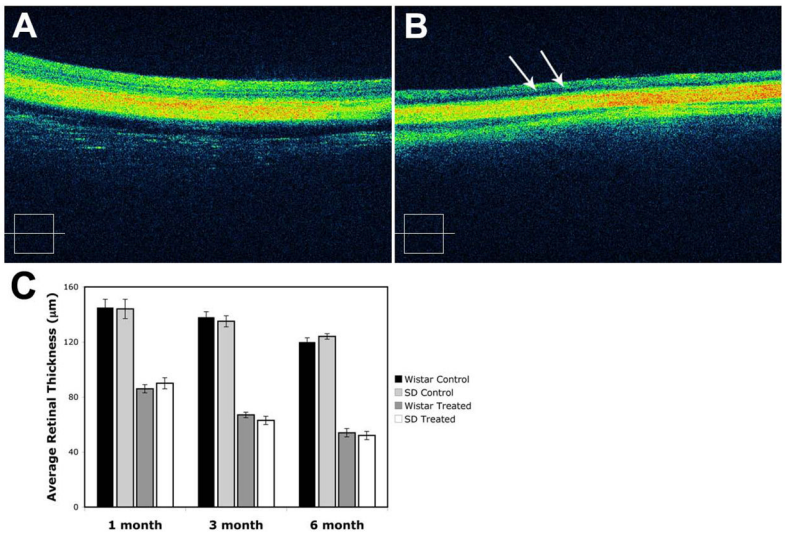

Figure 6.

OCT evaluation of Wistar rats after 6 months of intense cyclic light exposure. OCT retina scan from control Wistar rats showed that all the layers of retina are intact (A). OCT retina scan from intense light exposed Wistar rats showed the thinned retina with loss of photoreceptors, complete outer and partial inner nuclear layers (B). Hyporeflective intraretinal microcystic spaces (arrows) were also present. A representative image is shown. Similar patterns were observed in rats exposed to intense light after 1 or 3 months but to a lesser extent (not shown). The average retina thickness measurements, from internal limiting membrane to outer limiting membrane, are shown in C. A significant decrease in the average retina thickness in the light exposed Wistar and Sprague-Dawley rats was observed after 1, 3, or 6 month of intense light exposure, when compared to control group ($P < 0.05$; n=3).

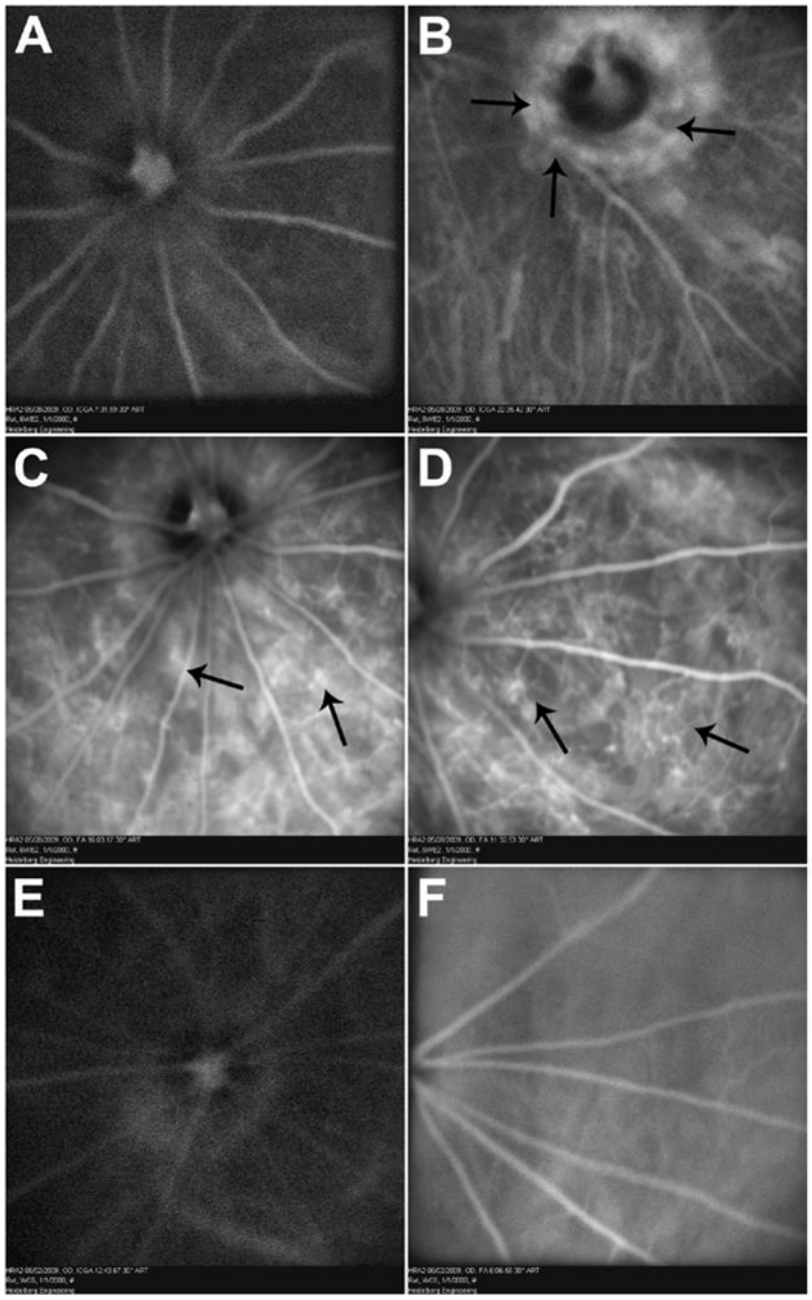

Figure 7.

ICG and fluorescence angiography of Wistar rats after 6 months of intense cyclic light exposure. Early phase (A) ICG angiography showing mild peripapillary hyperfluorescence increasing further in late phase (B) suggestive of peripapillary CNV (arrows). Intraretinal anastomosing new vessels, hypoperfused areas, and numerous focal hyperfluorescence areas of CNV (arrows) are seen on fluorescein angiography (C and D). Compared with fluorescein angiography, ICG improved visualization of choroidal circulation and enhanced visualization of some membranes that were poorly defined with fluorescein. In control groups, there are no foci of neovascularization or leakage on ICG (E) and fluorescein (F). Representative images are shown. All animals exposed to light exhibited a similar phenotype.

Table 1

Distinct histological features of Wistar and Sprague-Dawley rats after 1, 3, or 6 months of cyclic light exposure

	Changes were observed in all light-exposed animals			
Treated rats	**Neural Retina**	**RPE layer**	**Choroid**	**Bruch's membrane**
Wistar (1 month)	Total loss of inner and outer segments, outer nuclear layer reduced to less than 1/3 of original thickness	A few focal areas of proliferating RPE cells	Early formation of sub-RPE neovascularization	Intact
SD (1 month)	same as Wistar rats	same as Wistar rats	No areas of sub-RPE neovascularization were observed	Intact
Wistar (3 months)	Total loss of inner and outer segments and outer nuclear layer	Multiple areas of proliferating RPE cells	CNV formation in multiple areas	Breached in areas with proliferation of choroidal vessels
SD (3 months)	same as Wistar rats	Fewer areas of proliferating cells compared to Wistar rats	Only a few areas of sub-RPE neovascularization and early sub-retinal neovascularization were observed	Breached in a few areas
Wistar (6 months)	Total loss of inner and outer segments, and outer nuclear layer, inner nuclear layer was invaded and disrupted by invading fibrotic bands containing blood vessels	RPE cells growing into the overlying retina and extending to the ganglion cell layer	CNV formation with choroidal vessels extending to the ganglion cell layer; there was observable decrease in thickness of the choriocapillaris	Disrupted in multiple areas, PAS positive material deposition resembling drusen
SD (6 months)	Total loss of inner and outer segments, and outer nuclear layer; inner nuclear layer was thinned and areas invaded by occasional fibrotic bands containing blood vessels	RPE cells growing into the overlying inner nuclear layer and occasionally up to the ganglion cell layer	CNV formation with choroidal vessels growing towards ganglion cell layer, no appreciable decrease in choriocapillaris thickness	Areas of disruption were observed less frequently than in Wistar rats

Table 2

A comparison of the light-induced model with the existing transgenic and surgically intervened animal models producing retinal or choroidal neovascularization. (Adapted and modified from (6)).

Name	Genetic Modification/Surgical implantation	Features	References
Ccl2−/−	Ccl2−/− knockout mouse (MCP1 ; monocyte chemoattractant protein− 1)	lipofuscin, A2E, BLD, drusen, PR atrophy, CNV	(51,54,66, 67)
Ccr2−/−	Ccr2−/− knockout mouse (Ccr2; C- C chemokine receptor-2)		
Cp−/−Heph-/Y	Cp knockout mouse (Cp; ceruloplasmin) crossed with spontaneous sla mutation in C57BL/6 mice	PR and RPE atrophy, CNV	
rho/rtTA-TRE/VEGF	Transgenic, rhodopsin promoter driving inducible human VEGF expression		(68)
IRBP/rtTA-TRE/VEGF	Transgenic, IRBP (interphotoreceptor retinoid binding protein) promoter driving inducible human VEGF expression	retinal neovascularization	(69)
RPE65/VEGF	Transgenic, RPE65 promoter driving expression of murine VEGF	intrachoroidal neovascularization.	(70)
VLDLR (Vldlrtm1Her)	Vldlr−/− knockout mouse (Vldlr, very low density lipoprotein receptor)	choroidal anastomosis, retinal neovascularization	(52,71)
Matrigel model	Subretinal injection of Matrigel	RPE vacuolization and migration, inflammatory cell infiltrations within the Matrigel deposit, CNV	(72,73)
bFGF rabbit model	Subretinally implanted bFGF- impregnated gelatin microspheres	Subretinal neovascularization in 83% of their rabbit eyes	(74)
VEGF pellet implantation model	Intravitreous implantation of VEGF pellets	Transient retinal neovascularization	(75)
Light-induced rat model	No genetic or surgical manipulation, Chronic cyclic high intensity light exposure	RPE proliferation, BLD, sub-RPE neovascularization, CNV	

Abbreviations: A2E, N-retinylidene-N-retinylethanolamine; BLD, basal laminar/linear deposits; CNV, choroidal neovascularization; ERG, electroretinography; RPE, retinal pigment epithelial; PR, photoreceptor.